19. M. I. Bokarewa, M. Blomback, *Semin. Hematol.* **34**, 235 (1997).
20. D. K. Graham *et al.*, *Oncogene* **10**, 2349 (1995).
21. A. Neubauer *et al.*, *Blood* **84**, 1931 (1994).
22. A. Neubauer *et al. Leuk. Lymphoma*, **25**, 91 (1997).
23. Web figure 1 and supplemental text are available at *Science* Online at www.sciencemag.org/cgi/content/full/293/5528/306/DC1.
24. A. B. Lyons, C. R. Parish, *J. Immunol. Methods* **171**, 131 (1994).
25. B. Ernst *et al.*, *Immunity* **11**, 173 (1999).
26. Single-cell suspensions were prepared by Ficoll-Paque gradient centrifugation of cells collected from 1-2 wild-type spleens. Cells were washed twice, resuspended in PBS/0.1% bovine serum albumin (BSA) at a concentration of 1×10^7 cells/ml, and labeled with CFSE (5 μM) as described (*24*, *25*). Labeled cells were adjusted to 2×10^7/ml, and 300 μl of this suspension was injected intravenously into recipients' tail veins. Four to five days after injection, spleens and draining lymph nodes were collected, and single-cell suspensions were prepared for FACS sorting and analysis, as described above.
27. T. D. Camenisch *et al.*, *J. Immunol.* **162**, 3498 (1999).
28. R. S. Scott *et al.*, *Nature* **411**, 207 (2001).
29. Peritoneal macrophages were collected from 3% thioglycolate-treated mouse peritoneal cavities. After 2 hours of incubation in RPMI 1640 medium supplemented with 7% fetal bovine serum, unattached cells were washed off with culture medium and attached cells were cultured overnight. Phagocytosis assays were performed using a Vybrant Phagocytosis assay kit (Molecular Probes), as suggested by the manufacturer. Intracellular fluorescence at 520 nm was read on a Perkin-Elmer HTS7000plus bioassay reader.
30. M. Daëron, E. Vivier. *Curr. Topics Microbiol. Immunol.* **244**, 1 (1999).
31. The *Tyro 3* mutants were originally generated in our lab by M. Gore (currently at Arena Pharmaceuticals), with the assistance of R. Klein and his colleagues (EMBL). We thank S. Goff, G. Matsushima, and H. Shelton Earp for providing the *Axl* and *Mer* single mutants and D. Littman and C. Surh for critical review of earlier versions of the manuscript. Supported by grants from the NIH.

17 April 2001; accepted 11 June 2001

Regional Mu Opioid Receptor Regulation of Sensory and Affective Dimensions of Pain

Jon-Kar Zubieta,[1,2]* Yolanda R. Smith,[3] Joshua A. Bueller,[1] Yanjun Xu,[1] Michael R. Kilbourn,[2] Douglas M. Jewett,[2] Charles R. Meyer,[2] Robert A. Koeppe,[2] Christian S. Stohler[4]

The endogenous opioid system is involved in stress responses, in the regulation of the experience of pain, and in the action of analgesic opiate drugs. We examined the function of the opioid system and μ-opioid receptors in the brains of healthy human subjects undergoing sustained pain. Sustained pain induced the regional release of endogenous opioids interacting with μ-opioid receptors in a number of cortical and subcortical brain regions. The activation of the μ-opioid receptor system was associated with reductions in the sensory and affective ratings of the pain experience, with distinct neuroanatomical involvements. These data demonstrate the central role of the μ-opioid receptors and their endogenous ligands in the regulation of sensory and affective components of the pain experience.

Considerable advances have been made in the understanding of pronociceptive mechanisms at the level of their transduction, transmission, and central nervous system representation (*1–5*). At supraspinal levels, the development and widespread utilization of functional neuroimaging has allowed the examination of changes in the metabolic function of brain regions during the experience of pain. These data have consolidated the view that pain is a complex experience encompassing sensory, affective, and cognitive elements. Neuronal nuclei engaged in its sensory perception and localization, as well as those involved in its anticipatory and affective components, have been described as a result (*4–10*). However, the function of the supraspinal antinociceptive systems regulating the pain experience has not been sufficiently explored in humans. The existing data point to the presence of endogenous opioid release, a down-regulation of opioid receptors, or both, when patients diagnosed with persistent painful conditions have been studied before and after treatment with nonselective opioid receptor markers (*11–13*).

We examined the function of the endogenous opioid system and μ-opioid receptors during the experience of sustained pain in healthy human subjects. The μ-opioid receptors are implicated in antinociception, in stress-induced analgesia, and in the actions of exogenously administered opiate drugs (*14–19*). We studied 20 healthy volunteers, 13 men and 7 women, between the ages of 20 and 30 years (mean ± SD, 24 ± 2 years) (*20*) with positron emission tomography (PET) and [^{11}C]carfentanil, a selective μ-opioid receptor radiotracer (*21*, *22*). Each volunteer was studied twice, during experimentally induced sustained pain and during placebo administration applied in the masseter (jaw) muscles. Placebo and sustained painful challenges were introduced 20 min after radiotracer administration and were maintained for 20 min. Pain intensity was maintained constant (40 to 60 visual analog scale units) during that period of time (*23*). Pain and placebo conditions were administered in a double-blind, randomized and counterbalanced fashion. Parametric images of μ-opioid receptor binding potential (defined as the B_{max}/K_d for this receptor site) were then produced using data obtained from 20 to 70 min posttracer administration (*24*). Pain intensity was rated every 15 s, and its sensory and pain-specific affective qualities were rated after completion of the PET scans with the McGill Pain Questionnaire (MPQ) (*25*). Each participant also received a high-resolution magnetic resonance imaging (MRI) anatomical scan (*26*) that was coregistered to the PET parametric images of receptor binding potential (*27*).

From prior work in experimental animals, it was hypothesized that the painful condition would be associated with an increased release of endogenous opioids in the anterior and ventrolateral portions of the thalamus contralateral to the painful challenge (*28*, *29*), as well as in the ipsilateral amygdala (*30*). Under the experimental conditions used, the activation of the endogenous opioid system and μ-opioid receptors would be observed as reductions in μ-opioid receptor availability in vivo as measured with PET during the sustained pain condition, compared with placebo. Significant activations of the μ-opioid receptor system were detected in volumes of interest selected in the amygdala ipsilateral to the painful stimulus and in the contralateral ventrolateral portion of the thalamus. These data supported the initial hypothesis that the presence of sustained pain would induce a regionally selective release of endogenous opioids interacting with μ-opioid receptors, resulting in either competition with the radiolabeled tracer for the receptor sites, receptor internalization and recycling, or both (Table 1). The lateralization of these effects is also consistent with those observed in experimental animals (*28*, *30*).

In a second analysis, differences between pain and placebo conditions were tested for statistical significance on a pixel-by-pixel basis using statistical parametric mapping tech-

[1]Department of Psychiatry and Mental Health Research Institute, [2]Department of Radiology, [3]Department of Obstetrics and Gynecology, Medical School, and [4]Department of Biologic and Materials Sciences, School of Dentistry, The University of Michigan, Ann Arbor, MI 48104–1687, USA.

*To whom correspondence should be addressed. E-mail: zubieta@umich.edu

niques and SPM'99 software (*31*, *32*). Activations of the μ-opioid receptor system were detected in the dorsal anterior cingulate and lateral prefrontal cortex, bilaterally, in the insular cortex, thalamus, and hypothalamus contralateral to the painful challenge, and in the ipsilateral amygdala (Fig. 1). The binding potential values for the regions identified by this analysis, their stereotactic locations, cluster size, *z*-scores, and percent change from placebo to pain are shown in Table 2. The individual changes in μ-opioid receptor availability in vivo for the contralateral anterior thalamus are also shown in Fig. 1. Of note is the interindividual variability in μ-opioid receptor binding potential at baseline (placebo condition) and in the change in binding between conditions, reflecting the variability in the activation of the μ-opioid receptor system at similar levels of pain intensity, which was controlled for by the experimental paradigm (*23*).

These data demonstrate the activation of the μ-opioid receptor system under a physiological, controlled painful stimulus, directly in human subjects. The regional distribution of these activations coincides with that of studies examining the supraspinal representation of pain of short duration (*6*, *33–38*), or the effect of μ-opioid agonists on brain regional metabolic function (*39–41*).

The effects of the regional activation of the μ-opioid receptor system on the subjectively perceived pain experience were then examined. For this purpose, the sensory and affective scores of the MPQ subscales were correlated with the changes in μ-opioid receptor availability between conditions on a pixel-by-pixel basis with SPM'99. MPQ sensory ratings were negatively correlated with the degree of μ-opioid receptor system activation in the nucleus accumbens, thalamus, and amygdala ipsilateral to the painful challenge (Fig. 2). Correlations below the statistically significant level were observed in the periacqueductal gray (peak coordinates, –3, –29, –18, $z = 4.15$), a region also involved in μ-opioid receptor–mediated antinociception (*42*). The individual values for the change in μ-opioid receptor availability in relation with MPQ sensory scores for the ipsilateral amygdala and nucleus accumbens are shown in the graph insets of Fig. 2.

These findings are consistent with those of previous studies showing that the activation of amygdala μ-opioid receptors mediates antinociceptive responses, possibly through direct ipsilateral connections with the periacqueductal gray (*30*, *43*, *44*). The involvement of the ipsilateral thalamus in the representation of pain has also been described in studies

Table 1. Volume-of-interest analysis of endogenous opioid release during sustained masseter muscle pain. Volumes of interest (VOIs) were selected in the thalamus and the amygdala of each volunteer after alignment to the intercommisural line, but before anatomical normalization to stereotactic coordinates. The brain regions selected had been previously implicated in μ-opioid–mediated antinociception in animal models and were readily identifiable in the MR images. The thalamus was divided, on the basis of MRI landmarks, into anterior, posterior, dorsomedial, dorsolateral, ventromedial, and ventrolateral sections. Spheric volumes of identical size, 9 mm in diameter, were centered in the MR images in the anterior and ventrolateral divisions of the thalamus and in the amygdala, bilaterally, and then transferred to the coregistered μ-opioid receptor availability maps. Data are expressed as the means ± SD for each condition. Percent change refers to the percent average change (± SD) between B_{max}/K_d values obtained in the placebo and pain scans, within subjects.

Regions	Placebo (B_{max}/K_d)	Pain (B_{max}/K_d)	Percent change	*t* value	*P* value
Ipsilateral					
Amygdala	1.90 ± 0.43	1.77 ± 0.34	–5.1 ± 13.4	2.05	0.05*
Thalamus					
Anterior	2.13 ± 0.39	2.15 ± 0.37	1.5 ± 11.4	0.33	0.7
Ventrolateral	1.00 ± 0.18	1.01 ± 0.19	2.2 ± 13.2	0.57	0.6
Contralateral					
Amygdala	1.80 ± 0.33	1.75 ± 0.37	–2.1 ± 15.2	0.76	0.4
Thalamus					
Anterior	2.13 ± 0.47	2.02 ± 0.39	–3.5 ± 12.3	1.53	0.1
Ventrolateral	1.04 ± 0.27	0.96 ± 0.25	–7.1 ± 10.5	2.93	0.009*

*Significant changes in μ-opioid receptor availability in vivo from placebo to sustained pain. Paired, two-tailed *t*-tests, df = 19, $P < 0.05$.

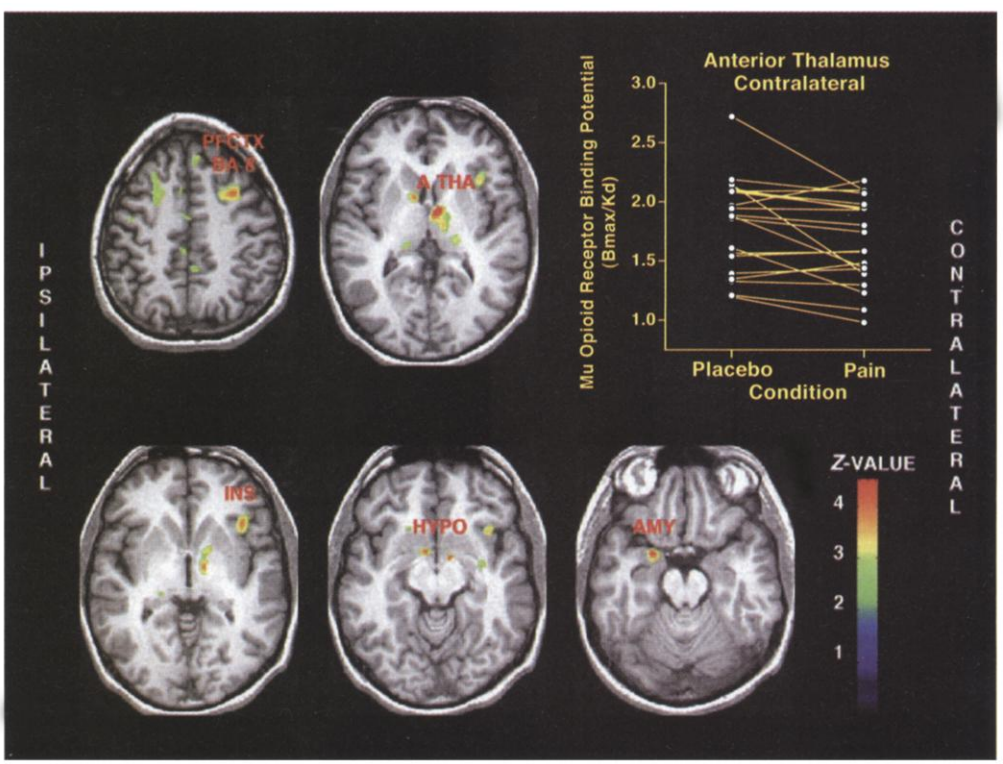

Fig. 1. Activation of the μ-opioid receptor system during sustained masseter muscle pain. Brain areas where significant reductions in regional μ-opioid receptor availability from placebo to sustained pain were obtained. *Z* scores of statistical significance are represented by the pseudocolor scale on the right of the image, and are superimposed over an anatomically standardized MRI image in axial views. Image data were prepared so that the left side of the image corresponds to the side where the painful stimulus was applied (ipsilateral). PFCTX BA 8, prefrontal cortex, Brodmann areas 8/9; A THA, anterior thalamus; INS, anterior insular cortex; HYPO, hypothalamus; AMY, amygdala.

examining supraspinal metabolic responses to tonic pain (*35*, *38*). In the case of the nucleus accumbens, this brain region has been most frequently associated with the mediation of reward reinforcement and in responses to novel environmental stimuli. However, there is recent evidence demonstrating its involvement in μ-receptor–mediated antinociception, perhaps through connections with the amygdala and the periacqueductal gray (*45*, *46*).

The activation of the μ-opioid receptor system during sustained pain was also negatively correlated with the pain-specific MPQ affective scores, bilaterally in the dorsal anterior cingulate cortex and thalamus, and ipsilaterally in the nucleus accumbens (Fig. 3). The values for the individual changes in receptor availability in the anterior cingulate and contralateral thalamus are shown in the graph insets of Fig. 3. These data support previous observations implicating the thalamus in experimental animals (*47*), and the dorsal anterior cingulate in humans (*8*, *48*), in

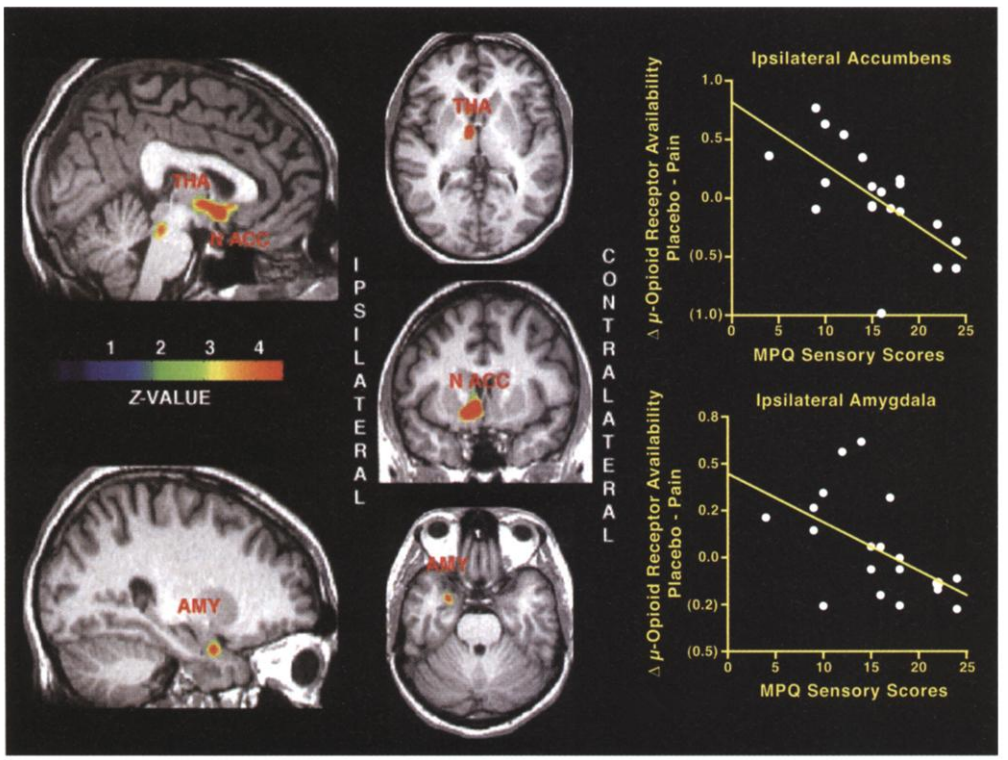

Fig. 2. Negative correlations between MPQ sensory scores and μ-opioid receptor system activation. Brain areas where significant correlations were obtained are shown, superimposed over an anatomically standardized MRI. *Z* scores of statistical significance are represented by the pseudocolor scale on the left. The thalamus, nucleus accumbens, and amygdala ipsilateral to the painful stimulus are shown in sagittal views, with *z*-scores of 8.66, 6.89, and 4.92, respectively (peak stereotactic coordinates, *x*, *y*, *z* in mm; thalamus, –7, –1, –1; nucleus accumbens, –10, 10, –8; amygdala, –27, 3, –26). In the right row, a detail of the correlations in the anterior thalamus, nucleus accumbens, and amygdala are shown in axial and coronal views. The graph insets show the individual changes in B_{max}/K_d values (placebo – pain) in the ipsilateral nucleus accumbens and amygdala plotted against MPQ sensory scores. AMY, amygdala; N ACC, nucleus accumbens; THA, anterior thalamus.

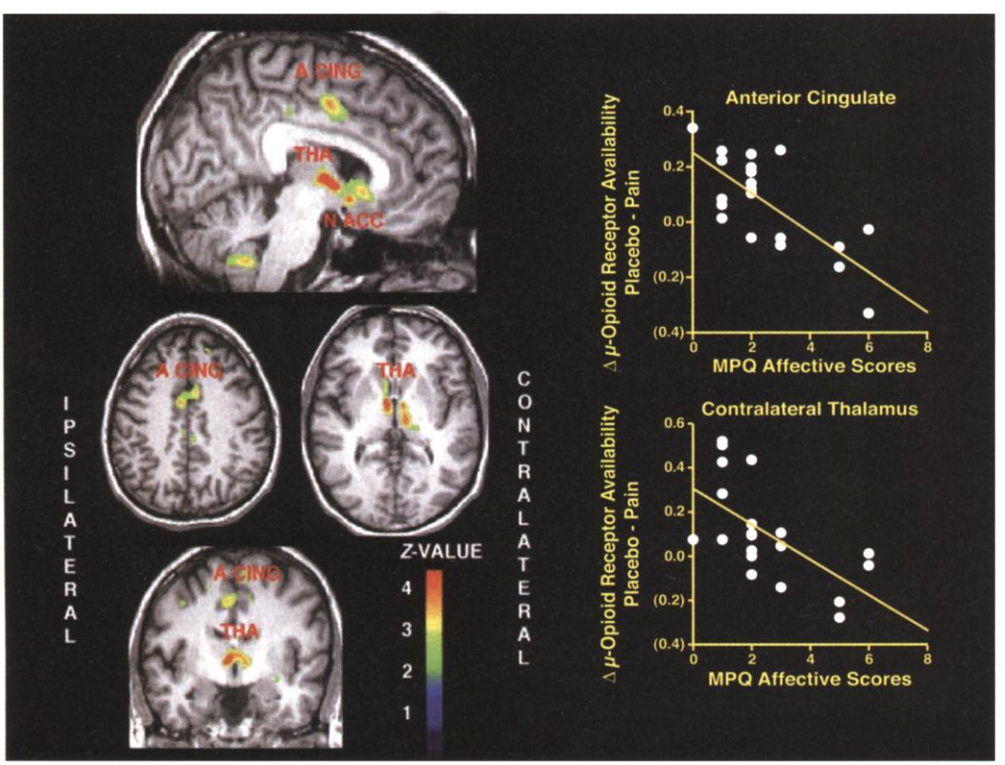

Fig. 3. Negative correlations between pain-specific MPQ affective scores and μ-opioid receptor system activation. Brain areas where significant correlations were found are shown, superimposed over an anatomically standardized MRI. *Z* scores of statistical significance are represented by the pseudocolor scale shown. In the upper figure, the anterior cingulate cortex (coordinates, *x*, *y*, *z* in mm, –8, –3, 46; $z = 4.11$, $P < 0.0001$ after correction for cluster volume and multiple comparisons), thalamus (ipsilateral, –7, –2, –1, $z = 5.76$, $P < 0.0001$; contralateral, 10, –16, 3, $z = 4.19$, $P < 0.001$), and ipsilateral nucleus accumbens (–8, 8, –9, $z = 4.44$, $P < 0.001$) are shown. Correlations that did not reach statistical levels of signficance were noted in the contralateral nucleus accumbens (11, 14, –6, $z = 4.24$, $P = 0.09$) and cerebellar vermis (–3, –49, –44, $z = 4.28$, $P = 0.08$). The lower three figures show details of some of these regions in axial and coronal views. The graph insets show the individual changes in B_{max}/K_d (placebo – pain) in the anterior cingulate and contralateral thalamus plotted against MPQ affective scores. A CING, anterior cingulate; THA, thalamus; N ACC, nucleus accumbens.

Table 2. Significant reductions in regional μ-opioid receptor availability in healthy human volunteers during sustained masseter muscle pain. Statistical parametric mapping analysis. Data represent the means ± SD of binding potential values in regions identified as showing significant reductions in μ-opioid receptor availability from placebo to sustained pain conditions in statistical parametric maps. Cluster size is expressed in 1^3-mm voxels. *Z* values refer to the comparison between placebo and pain B_{max}/K_d values, within subjects. Percent change refers to the percent average change (± SD) between B_{max}/K_d values obtained in the placebo and pain scans, within subjects. No significant increases in μ-opioid receptor availability were observed in the pain condition with respect to the placebo condition. C, contralateral to the side of pain; I, ipsilateral to the side of pain; (8/9), Brodmann areas 8/9 of the prefrontal cortex.

Regions	Placebo (B_{max}/K_d)	Pain (B_{max}/K_d)	Coordinates (*x*,*y*,*z*) (mm)	Cluster size (voxels)	*Z*	Percent change
Anterior thalamus (C)	1.81 ± 0.39	1.66 ± 0.36	6, −4, 4	604	5.06	−7.2 ± 12.0
Lateral thalamus (C)	1.11 ± 0.31	0.97 ± 0.25	15, −9, 15	306	4.83	−11.3 ± 13.9
Amygdala (I)	1.83 ± 0.44	1.70 ± 0.35	−24, 1, 19	468	4.55	−6.0 ± 11.1
Hypothalamus (C)	1.15 ± 0.49	1.02 ± 0.33	10, −2,−11	113	4.61	−3.9 ± 33.1
Significant after correction for cluster size						
Cingulate cortex	0.87 ± 0.14	0.77 ± 0.15	10,−24, 42	1335	3.49	−10.7 ± 12.7
Anterior insula (C)	1.09 ± 0.17	0.97 ± 0.19	39, 23, −2	1605	3.97	−10.5 ± 7.5
Prefrontal cortex (8/9) (I)	0.85 ± 0.15	0.75 ± 0.16	−20, −1,−59	1370	3.30	−11.0 ± 13.8
Prefrontal cortex (8/9) (C)	0.84 ± 0.15	0.73 ± 0.15	32, 9, 52	1876	4.17	−12.3 ± 13.0

the regulation of pain affect and unpleasantness. These results therefore indicate that the endogenous opioid system, through the activation of μ-opioid receptors in specific brain regions, is involved in the attenuation of sensory and pain-specific affective responses to a sustained painful stimulus. They also provide evidence for the role of this receptor in the regulation of the individual experience of pain.

Multiple cortical and subcortical brain regions appear involved in μ-opioid–mediated antinociceptive responses. As has been described by other authors (*4*, *5*, *9*, *29*, *47*, *49*), some regions demonstrated specialized functions, regulating primarily sensory (e.g., ipsilateral nucleus accumbens and amygdala) or affective (e.g., anterior cingulate) components of the pain experience. Conversely, the activation of μ-opioid receptors in the thalamus appeared to regulate both these dimensions, possibly through local and thalamocortical pathways impacting somatosensory, affective, and cognitive aspects of the pain experience (*28*, *29*, *47*, *49*).

The ability to examine the function of specific neurotransmitter systems directly in human subjects has important implications for the study of physiological and pathological brain processes. In the case of the μ-opioid receptor and its endogenous ligands, the study of interindividual differences in μ-receptor–mediated antinociceptive and stress responses is highly relevant to the understanding of the variability in the experience of pain across subjects. In this regard, the function of the opioid receptor system is influenced by gender, gonadal steroids, and the presence of persistent pain (*11–13*, *50–52*). Further investigation of these phenomena appears warranted due to their direct implications for the understanding and treatment of persistent pain syndromes, a serious health concern with considerable morbidity for the individual and substantial costs to society.

References and Notes

1. M. J. Caterina *et al.*, *Science* **288**, 306 (2000).
2. P. W. Mantyh *et al.*, *Science* **278**, 275 (1997).
3. A. B. Malmberg, C. Chen, S. Tonegawa, A. I. Basbaum, *Science* **278**, 279 (1997).
4. D. D. Price, *Science* **288**, 1769 (2000).
5. R.-D. Treede, D. R. Kenshalo, R. H. Gracely, A. K. P. Jones, *Pain* **79**, 105 (1999).
6. J. Talbot *et al.*, *Science* **251**, 1355 (1991).
7. A. Craig, E. Reiman, A. Evans, M. Bushnell, *Nature* **384**, 258 (1996).
8. P. Rainville, G. H. Duncan, D. D. Price, B. Carrier, M. C. Bushnell, *Science* **277**, 968 (1997).
9. K. Casey, *Proc. Natl. Acad. Sci. U.S.A.* **96**, 7668 (1999).
10. A. Ploghaus *et al.*, *Science* **284**, 1979 (1999).
11. A. Jones *et al.*, *Br. J. Rheumatol.* **33**, 909 (1994).
12. A. Jones *et al.*, *J. Cereb. Blood Flow Metab.* **19**, 803 (1999).
13. F. Willoch *et al.*, *AJNR Am. J. Neuroradiol.* **20**, 686 (1999).
14. H. Akil *et al.*, *Annu. Rev. Neurosci.* **7**, 223 (1984).
15. M. Rubinstein *et al.*, *Proc. Natl. Acad. Sci. U.S.A.* **93**, 3995 (1996).
16. C. La Buda, I. Sora, G. Uhl, P. Fuchs, *Brain Res.* **869**, 1 (2000).
17. C. Wiedenmayer, G. Barr, *Behav. Neurosci.* **114**, 125 (2000).
18. H. W. D. Matthes *et al.*, *Nature* **383**, 819 (1996).
19. I. Sora *et al.*, *Proc. Natl. Acad. Sci. U.S.A* **94**, 1544 (1997).
20. Volunteers were healthy right-handed men and women with an educational level 18 ± 2 years, nonsmokers, who had no personal history of medical illness, psychiatric illness, substance abuse, or dependence, and no family history of inheritable illnesses. Volunteers were not taking psychotropic medications or hormonal treatments. Women had not used hormonal birth control for at least 6 months, and were scanned during the follicular phase of their menstrual cycles (2 to 9 days after the onset of menses), as ascertained by plasma levels of estradiol (47 ± 32 ng/ml) and progesterone (<1 ng/ml in all cases). To further standardize the hormonal millieu of the women volunteers, the presence of ovulatory cycles before scanning was also determined by a progesterone level of >3 ng/ml during the luteal phase of the preceding menstrual cycle. All procedures were approved by the University of Michigan Investigational Review Boards.
21. J. Frost *et al.*, *J. Comput. Assist. Tomog.* **9**, 231 (1985).
22. M. Titeler *et al.*, *Eur. J. Pharmacol.* **167**, 221 (1989).
23. X. Zhang, J. A. Ashton-Miller, C. S. Stohler, *IEEE Trans. Biomed. Eng.* **40**, 344 (1993).
24. PET scans were acquired with a Siemens ECAT EXACT scanner in three dimensional mode with septa retracted. Participants were positioned in the PET scanner gantry, and two intravenous (*antecubital*) lines were placed. A light forehead restraint was used to eliminate intrascan movement. [^{11}C]carfentanil was synthesized at high specific activity (>1000 Ci/mmol) by the reaction of ^{11}C-methyliodide and a nonmethyl precursor as previously described (*53*) with minor modifications to improve its synthetic yield; 10 to 15 mCi (370–555 MBq) were administered to each subject for each of the two PET scans. The two administrations were separated by 2 hours to allow for tracer decay. The maximum mass of carfentanil injected was 0.03 μg/kg per study, ensuring that the compound was administered in tracer quantities, i.e., subpharmacological doses. Fifty-five percent of the [^{11}C]carfentanil dose was administered as a bolus and the remainder as a continuous infusion using a computer-controlled pump to achieve steady-state tracer levels. Nineteen sets of scans were acquired over 70 min with an increasing duration (30 s up to 10 min). Images were reconstructed using filtered back-projection with a Hanning 0.5 filter, and included both measured attenuation and scatter corrections. Dynamic images were coregistered to each other and the intercommisural line using automated computer routines (*54*). Image data were then transformed on a pixel-by-pixel basis into two sets of parametric maps: (a) a tracer transport measure (K_1 ratio), and (b) a receptor-related measure, distribution volume ratio (DVR). To avoid the need for arterial blood sampling, the tracer transport and binding measures were calculated using a modified Logan graphical analysis (*55*), using the occipital cortex (an area devoid of μ-opioid receptors) as the reference region. With the protocol used, the Logan plot becomes linear by 10 min after the start of radiotracer administration, with its slope being the DVR, a measure equal to the (B_{max}/K_d) + 1 for this receptor site and radiotracer. B_{max}/K_d (or DVR-1) is the "receptor related" measure (μ-opioid receptor availability, or binding potential). K_1 and DVR images for each experimental period and MR images were coregistered to each other and to the International Consortium for Brain Mapping (ICBM) stereotactic atlas orientation (*27*).
25. R. Melzack, J. Katz, in *Handbook of Pain Assessment*, D. Turk, R. Melzack, Eds. (Guilford Press, New York, 2000) pp. 152–168.
26. MRI scans were acquired on a 1.5 Tesla scanner (Signa, General Electric, Milwaukee, WI). Acquisition sequences were axial SPGR IR-Prep MR (TE = 5.5, TR = 14, TI = 300, flip angle = 20°, NEX = 1, 124 contiguous images, 1.5 mm thickness), followed by axial T2 and proton density images (TR = 4000, TE = 20 and 100, respectively, NEX = 1, 62 contiguous images, 3 mm thick). All MR scans were reviewed by a neuroradiologist to rule out gross structural brain abnormalities before PET scanning.
27. C. R. Meyer *et al.*, *Med. Image Anal.* **1**, 195 (1997).
28. D. Albe-Fessard, K. J. Berkley, L. Kruger, H. J. Ralston, W. D. Willis, *Brain Res. Rev.* **9**, 217 (1985).
29. M. C. Bushnell, G. H. Duncan, *Exp. Brain Res.* **78**, 415 (1989).
30. B. Manning, *J. Neurosci.* **18**, 9453 (1998).
31. Parametric maps of differences between conditions (pain-placebo) were generated by anatomically standardizing the MRI of each subject to the International Conference on Brain Mapping (ICBM) stereotactic atlas coordinates, with subsequent application of this transformation to the μ-opioid receptor binding maps (*27*). Before nonlinear warping, image data were prepared so that the side of the painful challenge (induced on the right or the left masseter muscle, in a counterbalanced design) was located on the same side of the image for all subjects. Image data are therefore presented as "ipsilateral" or "contralateral" to the painful stimulus, regardless of the actual location (right-left). Differences between conditions and subject groups were then mapped into stereotactic space using *z*-maps of statistical significance with SPM'99 and Matlab software and using a general linear model and correction for multiple comparisons (*56*), but without global normalization (the

data presented are based on absolute B_{max}/K_d estimates). Only regions with specific μ-opioid receptor binding were included in the analyses (pixels with DVR values >1.2 times the mean global image value for μ-opioid receptor images as calculated with SMP'99). To compensate for small residual anatomic variations across subjects and to improve signal to noise ratios, a three-dimensional Gaussian filter (FWHM 6 mm) is applied to each scan. For each subtraction analysis of one sample, two-tailed *t*-statistic values were calculated for each pixel using the pooled variance across pixels (*57*). Areas of significant differences were detected using a statistical threshold that controls a type 1 error rate at $P = 0.05$ for multiple comparisons, which was estimated using the Euler characteristic (*57*) based on the number of pixels in the gray matter and image smoothness (*58*). This typically varies from $z = 4.4$ to 4.6 in our studies for peak analyses, at a final resolution of approximately 10 mm. *Z* scores were also deemed significant if they reached statistical thresholds after correction for the size of the cluster under consideration (*32*).

32. K. J. Friston, K. J. Worsley, R. S. J. Frackowiak, J. C. Mazziotta, A. C. Evans, *Hum. Brain Map.* **1**, 210 (1994).
33. R. Coghill *et al.*, *J. Neurosci.* **14**, 4095 (1994).
34. A. K. Jones, W. D. Brown, K. J. Friston, L. Y. Qi, R. S. Frackowiak, *Proc. R. Soc. London Ser. B* **244**, 39 (1991).
35. K. Casey, S. Minoshima, T. Morrow, R. Koeppe, *J. Neurophysiol.* **76**, 571 (1996).
36. D. Silverman *et al.*, *Gastroenterology* **112**, 64 (1997).
37. Q. Aziz *et al.*, *Gastroenterology* **113**, 50 (1997).
38. S. Derbyshire, A. Jones, *Pain* **76**, 127 (1998).
39. T. Schlaepfer *et al.*, *Am. J. Psychiatry* **155**, 470 (1998).
40. L. J. Adler *et al.*, *Anesth. Analg.* **84**, 120 (1997).
41. K. Casey *et al.*, *J. Neurophysiol.* **84**, 525 (2000).
42. H. Fields, M. Heinricher, P. Mason, *Annu. Rev. Neurosci.* **14**, 219 (1991).
43. F. J. Helmstetter, P. S. Bellgowan, L. H. Poore, *J. Pharmacol. Exp. Ther.* **275**, 381 (1995).
44. S. Tershner, F. Helmstetter, *Brain Res.* **865**, 17 (2000).
45. R. Gear, J. Levine, *J. Neurosci.* **15**, 3154 (1995).
46. R. Gear, K. Aley, J. Levine, *J. Neurosci.* **19**, 7175 (1999).
47. S. Harte, A. Lagman, G. Borszcz, *Brain Res.* **874**, 78 (2000).
48. T. Tolle *et al.*, *Ann. Neurol.* **45**, 40 (1999).
49. K. Carr, T. Bak, *Brain Res.* **441**, 173 (1988).
50. S. Tershner, J. Mitchell, H. Fields, *Pain* **85**, 153 (2000).
51. J. Zubieta, R. Dannals, J. Frost, *Am. J. Psychiatry* **156**, 842 (1999).
52. Y. Smith *et al.*, *J. Clin. Endocrinol. Metab.* **83**, 4498 (1998).
53. R. Dannals *et al.*, *Int. J. Appl. Radiat. Isot.* **36**, 303 (1985).
54. S. Minoshima *et al.*, *Nucl. Med.* **34**, 322 (1993).
55. J. Logan *et al.*, *J. Cereb. Blood Flow Metab.* **16**, 834 (1996).
56. K. J. Friston *et al.*, *Hum. Brain Map.* **2**, 189 (1995).
57. K. Worsley, A. Evans, S. Marrett, P. Neelin, *J. Cereb. Blood Flow Metab.* **12**, 900 (1992).
58. K. J. Friston, C. D. Frith, P. F. Liddle, R. S. J. Frackowiak, *J. Cereb. Blood Flow Metab.* **11**, 690 (1991).
59. Supported by grants R01 DE 12743 to J.-K.Z. and R01 DE 12059 to C.S.S. The authors also wish to acknowledge C. J. Kowalski for helpful discussions and statistics support and the Nuclear Medicine Technologists of the PET Center at the University of Michigan who aided in the acquisition and reconstruction of the PET studies.

22 March 2001; accepted 1 June 2001